Available online at www.sciencedirect.com
SCIENCE DIRECT®
PHYSICS LETTERS B
ELSEVIER
Physics Letters B 567 (2003) 243–250
www.elsevier.com/locate/npe

# Full transverse-momentum spectra of low-mass Drell–Yan pairs at LHC energies

George Fai [a], Jianwei Qiu [b], Xiaofei Zhang [a]

[a] *Center for Nuclear Research, Department of Physics, Kent State University, Kent, OH 44242, USA*
[b] *Department of Physics and Astronomy, Iowa State University, Ames, IA 50011, USA*

Received 5 March 2003; accepted 23 May 2003

Editor: W. Haxton

**Abstract**

The transverse momentum distribution of low-mass Drell–Yan pairs is calculated in QCD perturbation theory with all-order resummation. We argue that at LHC energies the results should be reliable for the entire transverse momentum range. We demonstrate that the transverse momentum distribution of low-mass Drell–Yan pairs is an advantageous source of constraints on the gluon distribution and its nuclear dependence.
© 2003 Elsevier B.V. Open access under CC BY license.

## 1. Introduction

Dilepton production in hadronic collisions is an excellent laboratory for the investigations of strong interaction dynamics. This channel provides an opportunity for discovery of quarkonium states and a clean process for the study of parton distribution functions (PDF). In the Drell–Yan process, the massive lepton-pair is produced via the decay of an intermediate $Z^0$ boson or a virtual photon $\gamma^*$ with mass $M$. When $M \sim M_Z$, the high mass dilepton production in heavy ion collisions at LHC energies is dominated by the $Z^0$ channel and is an excellent hard probe of QCD dynamics [1]. In this Letter, we demonstrate that the transverse momentum distribution of low-mass ($\Lambda_{\rm QCD} \ll M \ll M_Z$) dilepton production at LHC energies is a reliable probe of both hard and semihard physics at LHC energies and is an advantageous source of constraints on gluon distribution in the proton and in nuclei. In addition, it provides an important contribution to dilepton spectra at the LHC, which is the appropriate channel to study $J/\psi$, heavy quarks etc.

## 2. Full $p_{\rm T}$ spectrum of low-mass Drell–Yan pairs

In Drell–Yan production, if both, the physically measured dilepton mass $M$ and the transverse momentum $p_{\rm T}$ are large, the cross section in a collision between hadrons (or nuclei) $A$ and $B$, $A(P_A) + B(P_B) \to \gamma^*(\to l\bar{l}) + X$, can be factorized systematically in QCD perturbation theory and expressed as [2]

$$\frac{d\sigma_{AB\to l\bar{l}(M)X}}{dM^2\,dy\,dp_{\rm T}^2}$$

*E-mail address:* fai@cnr8.physics.kent.edu (G. Fai).

0370-2693 © 2003 Elsevier B.V. Open access under CC BY license.
doi:10.1016/j.physletb.2003.05.007

$$= \left(\frac{\alpha_{\rm em}}{3\pi M^2}\right) \sum_{a,b} \int dx_1\, \phi_{a/A}(x_1,\mu) \times \int dx_2\, \phi_{b/B}(x_2,\mu) \times \frac{d\hat{\sigma}_{ab\to\gamma^* X}}{dp_{\rm T}^2\, dy}(x_1,x_2,M,p_{\rm T},y;\mu). \quad (1)$$

The sum $\sum_{a,b}$ runs over all parton flavors; $\phi_{a/A}$ and $\phi_{b/B}$ are normal parton distributions; and $\mu$ represents the renormalization and factorization scales. The $d\hat{\sigma}_{ab\to\gamma^* X}/dp_{\rm T}^2\, dy$ in Eq. (1) is the short-distance probability for partons of flavors $a$ and $b$ to produce a virtual photon of invariant mass $M$ and is calculable perturbatively in terms of a power series in $\alpha_s(\mu)$. The scale $\mu$ is of the order of the energy exchange in the reaction, $\mu \sim \sqrt{M^2 + p_{\rm T}^2}$.

The transverse momentum ($p_{\rm T}$) distribution of the dileptons can be divided into three regions: low-$p_{\rm T}$ ($\ll M$), intermediate-$p_{\rm T}$ ($\sim M$), and high-$p_{\rm T}$ ($\gg M$) regions. When both the physically measured $M$ and $p_{\rm T}$ are large and are of the same order, the short-distance partonic part $d\hat{\sigma}_{ab\to\gamma^* X}/dp_{\rm T}^2\, dy$ in Eq. (1) can be calculated reliably in conventional fixed-order QCD perturbation theory in terms of a power series in $\alpha_s(\mu)$. However, when $p_{\rm T}$ is very different from $M$, the calculation of Drell–Yan production in both low and high-$p_{\rm T}$ regions becomes a two-scale problem in perturbative QCD, and the calculated partonic parts include potentially large logarithmic terms proportional to a power of $\ln(M/p_{\rm T})$. As a result, the higher order corrections in powers of $\alpha_s$ are not necessary small. The ratio $\sigma^{\rm NLO}/\sigma^{\rm LO}$ [$\propto \alpha_s \times$ (large logarithms)] can be of order 1, and convergence of the conventional perturbative expansion in powers of $\alpha_s$ is possibly impaired.

In the low-$p_{\rm T}$ region, there are two powers of $\ln(M^2/p_{\rm T}^2)$ for each additional power of $\alpha_s$, and the Drell–Yan $p_{\rm T}$ distribution calculated in fixed-order QCD perturbation theory is known not to be reliable. Only after all-order resummation of the large $\alpha_s^n \ln^{2n+1}(M^2/p_{\rm T}^2)$ do predictions for the $p_{\rm T}$ distributions become consistent with data [3,4]. We demonstrate in Section 3 that low-mass Drell–Yan production at $p_T$ as low as $\Lambda_{\rm QCD}$ at LHC energies can be calculated reliably in perturbative QCD with all order resummation.

When $p_{\rm T} \geqslant M/2$, the lowest-order virtual photon "Compton" subprocess: $g + q \to \gamma^* + q$ dominates the $p_{\rm T}$ distribution, and the high-order contributions including all-order resummation of $\alpha_s^n \ln^{n-1}(M^2/p_{\rm T}^2)$ preserve the fact that the $p_{\rm T}$ distributions of low-mass Drell–Yan pairs are dominated by gluon initiated partonic subprocesses [5]. We show in Section 4 that the $p_{\rm T}$ distribution of low-mass Drell–Yan pairs can be a good probe of the gluon distribution and its nuclear dependence. We give our conclusions in Section 5.

## 3. Low transverse momentum region

Resummation of large logarithmic terms at low $p_{\rm T}$ can be carried out in either $p_{\rm T}$ or impact parameter ($b$) space, which is the Fourier conjugate of $p_{\rm T}$ space. All else being equal, the $b$ space approach has the advantage that transverse momentum conservation is explicit. Using renormalization group techniques, Collins, Soper, and Sterman (CSS) [6] devised a $b$ space resummation formalism that resums all logarithmic terms as singular as $(1/p_{\rm T}^2)\ln^m(M^2/p_{\rm T}^2)$ when $p_{\rm T} \to 0$. This formalism has been used widely for computations of the transverse momentum distributions of vector bosons in hadron reactions [7].

At low-mass $M$, Drell–Yan transverse momentum distributions calculated in the CSS $b$-space resummation formalism strongly depend on the non-perturbative parameters at fixed target energies. However, it was pointed out recently that the predictive power of perturbative QCD (pQCD) resummation improves with total center-of-mass energy ($\sqrt{s}$), and when the energy is high enough, pQCD should have good predictive power even for low-mass Drell–Yan production [3]. The LHC will provide us a chance to study low-mass Drell–Yan production at unprecedented energies.

In the CSS resummation formalism, the differential cross section for Drell–Yan production in Eq. (1) is reorganized as the sum

$$\frac{d\sigma_{AB\to l\bar{l}(M)X}}{dM^2\, dy\, dp_{\rm T}^2} = \frac{d\sigma^{(\rm resum)}_{AB\to l\bar{l}(M)X}}{dM^2\, dy\, dp_{\rm T}^2} + \frac{d\sigma^{(\rm Y)}_{AB\to l\bar{l}(M)X}}{dM^2\, dy\, dp_{\rm T}^2}. \quad (2)$$

The all-orders resummed term is a Fourier transform from the $b$-space,

$$\frac{d\sigma^{(\mathrm{resum})}_{AB\to l\bar{l}(M)X}}{dM^2\,dy\,dp_{\mathrm{T}}^2} = \frac{1}{(2\pi)^2}\int d^2b\, e^{i\vec{p}_{\mathrm{T}}\cdot\vec{b}} W(b,M,x_A,x_B) = \frac{1}{2\pi}\int db\, J_0(p_{\mathrm{T}}b) b W(b,M,x_A,x_B), \tag{3}$$

where $J_0$ is a Bessel function, $x_A = e^{y}M/\sqrt{s}$ and $x_B = e^{-y}M/\sqrt{s}$, with rapidity $y$ and collision energy $\sqrt{s}$. In Eq. (2), the $\sigma^{(\mathrm{resum})}$ term dominates the $p_{\mathrm{T}}$ distributions when $p_{\mathrm{T}} \ll M$, and the $\sigma^{(\mathrm{Y})}$ term gives corrections that are negligible for small $p_{\mathrm{T}}$, but become important when $p_{\mathrm{T}} \sim M$.

The function $W(b,M,x_A,x_B)$ resums to all orders in QCD perturbation theory the singular terms that would otherwise behave as $\delta^2(p_{\mathrm{T}})$ and $(1/p_{\mathrm{T}}^2)\times \ln^m(M^2/p_{\mathrm{T}}^2)$ in transverse momentum space, for all $m \geqslant 0$, and can be calculated perturbatively for small $b$,

$$W(b,M,x_A,x_B) = \mathrm{e}^{-S(b,M)} W(b,c/b,x_A,x_B) \equiv W^{\mathrm{pert}}(b,M,x_A,x_B), \tag{4}$$

where all large logarithms from $\ln(c^2/b^2)$ to $\ln(M^2)$ have been completely resummed into the exponential factor

$$S(b,M) = \int_{c^2/b^2}^{M^2} \frac{d\mu^2}{\mu^2}\big[\ln\big(M^2/\mu^2\big)\mathcal{A}(\alpha_s(\mu)) + \mathcal{B}(\alpha_s(\mu))\big],$$

with functions $\mathcal{A}$ and $\mathcal{B}$ given in Ref. [6], and $c = 2e^{-\gamma_{\mathrm{E}}}$ with Euler's constant $\gamma_{\mathrm{E}} \approx 0.577$. The function $W(b,c/b,x_A,x_B)$ in Eq. (4) is given in terms of modified parton distributions from hadron $A$ and $B$ [6]. With only one large momentum scale $1/b$, $W(b,c/b,x_A,x_B)$ is perturbatively calculable. Since the perturbatively resummed $W^{\mathrm{pert}}(b,M,x_A,x_B)$ in Eq. (4) is only reliable for the small $b$ region, an extrapolation to the nonperturbative large $b$ region is necessary in order to complete the Fourier transform in Eq. (3).

In the original CSS formalism, a variable $b_*$ and a nonperturbative function $F^{\mathrm{NP}}_{\mathrm{CSS}}(b,M,x_A,x_B)$ were introduced to extrapolate the perturbatively calculated $W^{\mathrm{pert}}$ into the large $b$ region such that the full $b$-space distribution was of the form

$$W^{\mathrm{CSS}}(b,M,x_A,x_B) \equiv W^{\mathrm{pert}}(b_*,M,x_A,x_B) \times F^{\mathrm{NP}}_{\mathrm{CSS}}(b,M,x_A,x_B), \tag{5}$$

where $b_* = b/\sqrt{1+(b/b_{\max})^2}$, with $b_{\max} = 0.5\ \mathrm{GeV}^{-1}$. This construction ensures that $b_* \leqslant b_{\max}$ for all values of $b$.

In terms of the $b_*$ formalism, a number of functional forms for the $F^{\mathrm{NP}}_{\mathrm{CSS}}$ have been proposed. A simple Gaussian form in $b$ was first proposed by Davies, Webber, and Stirling (DWS) [8],

$$F^{\mathrm{NP}}_{\mathrm{DWS}}(b,M,x_A,x_B) = \exp\big\{-(g_1+g_2\ln(M/2M_0))b^2\big\}, \tag{6}$$

with the parameters $M_0 = 2$ GeV, $g_1 = 0.15\ \mathrm{GeV}^2$, and $g_2 = 0.4\ \mathrm{GeV}^2$. In order to take into account the apparent dependence on collision energies, Ladinsky and Yuan (LY) introduced a new functional form [9],

$$F^{\mathrm{NP}}_{\mathrm{LY}}(b,M,x_A,x_B) = \exp\big\{-(g_1+g_2\ln(M/2M_0))b^2 - g_1g_3\ln(100x_Ax_B)b\big\}, \tag{7}$$

with $M_0 = 1.6$ GeV, $g_1 = 0.11^{+0.04}_{-0.03}\ \mathrm{GeV}^2$, $g_2 = 0.58^{+0.1}_{-0.2}\ \mathrm{GeV}^2$, and $g_3 = -1.5^{+0.1}_{-0.1}\ \mathrm{GeV}^{-1}$. Recently, Landry, Brook, Nadolsky, and Yuan proposed a modified Gaussian form [10],

$$F^{\mathrm{NP}}_{\mathrm{BLNY}}(b,M,x_A,x_B) = \exp\big\{-\big[g_1+g_2\ln(M/2M_0) + g_1g_3\ln(100x_Ax_B)\big]b^2\big\}, \tag{8}$$

with $M_0 = 1.6$ GeV, $g_1 = 0.21^{+0.01}_{-0.01}\ \mathrm{GeV}^2$, $g_2 = 0.68^{+0.01}_{-0.02}\ \mathrm{GeV}^2$, and $g_3 = -0.6^{+0.05}_{-0.04}$. All these parameters were obtained by fitting low energy Drell–Yan and high energy $W$ and $Z$ data. Note, however that the $b_*$ formalism introduces a modification to the perturbative calculation, and the size of the modifications strongly depends on the nonperturbative parameters in $F^{\mathrm{NP}}(b,M,x_A,x_B)$, the intermediate boson mass $M$, and collision energy $\sqrt{s}$ [7].

A remarkable feature of the $b$-space resummation formalism is that the resummed exponential factor $\exp[-S(b,M)]$ suppresses the $b$-integral when $b$ is larger than $1/M$. It can be shown using the saddle

point method that, for a large enough $M$, QCD perturbation theory is valid even at $p_T = 0$ [6]. For high energy heavy boson ($W$, $Z$, and Higgs) production, the integrand of $b$-integration in Eq. (3) at $p_T = 0$ is proportional to $bW(b, Q, x_A, x_B)$, which has a saddle point $b_{sp}$ well within the perturbative region ($b_{sp} < b_{max}$), and therefore, the $b$-integration in Eq. (3) is dominated by the perturbatively resummed calculation. The uncertainties from the large-$b$ region have very little effect on the calculated $p_T$ distributions, and the resummation formalism is of a good predictive power.

On the other hand, in the low energy Drell–Yan production, there is no saddle point in the perturbative region for the integrand in Eq. (3), and therefore the dependence of the final result on the nonperturbative input is strong [3,4]. However, as discussed in Refs. [3, 7,11], the value of the saddle point strongly depends on the collision energy $\sqrt{s}$, in addition to its well-known $M^2$ dependence.

Fig. 1 shows the integrand of the $b$-integration in Eq. (3) at $p_T = 0$ for production of Drell–Yan pairs of mass $M = 5$ GeV in proton–proton collisions at $\sqrt{s} = 5.5$ TeV and $b_{max} = 0.5$ GeV$^{-1}$. Different curves represent different extrapolations to the large-$b$ region. The three curves (dashed, dotted, and dot-dashed) are evaluated using the $b_*$ formalism with the DWS, LY, and BLNY nonperturbative functions, respectively. Although these three nonperturbative functions give similar $b$-space distributions for heavy boson production at Tevatron energies, they predict very different $b$-space distributions for low-mass Drell–Yan production at LHC energies even within the perturbative small-$b$ region. Since the $b$-distribution in Fig. 1 completely determines the resummed $p_T$ distribution through the $b$-integration weighted by the Bessel function $J_0(p_T b)$, we need to be concerned with the uncertainties of the resummed low-mass $p_T$ distributions calculated with different nonperturbative functions. We use the CTEQ5M parton distribution function [12] throughout.

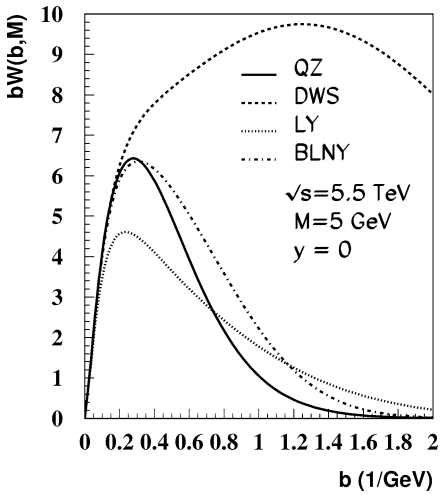


Fig. 1. The $b$-space resummed functions $bW(b)$ in Eq. (3) for Drell–Yan production of dilepton mass $M = 5$ GeV at $\sqrt{s} = 5.5$ TeV with the ZQ (solid), DWS (dashed), LY (dotted), and BNLY (dot-dashed) formalism of nonperturbative extrapolation.

In order to improve the situation, a new formalism of extrapolation (QZ) was proposed [3],

$$W(b, M, x_A, x_B) = \begin{cases} W^{\text{pert}}(b, M, x_A, x_B), & b \leqslant b_{\max}, \\ W^{\text{pert}}(b_{\max}, M, x_A, x_B) \\ \quad \times F^{\text{NP}}(b, M, x_A, x_B; b_{\max}, \alpha), & b > b_{\max}, \end{cases} \tag{9}$$

where the nonperturbative function $F^{\text{NP}}$ is given by

$$F^{\text{NP}} = \exp\Big\{ -\ln\big(M^2 b_{\max}^2/c^2\big)\Big[g_1\big((b^2)^\alpha - \big(b_{\max}^2\big)^\alpha\big) + g_2\big(b^2 - b_{\max}^2\big)\Big] - \bar{g}_2\big(b^2 - b_{\max}^2\big)\Big\}. \tag{10}$$

Here, $b_{\max}$ is a parameter to separate the perturbatively calculated part from the nonperturbative input, and its role is similar to the $b_{\max}$ in the $b_*$ formalism. The term proportional to $g_1$ in Eq. (10) represents a direct extrapolation of the resummed leading power contribution to the large $b$ region; and the parameters $g_1$ and $\alpha$ are determined by the continuity of the function $W(b, M, x_A, x_B)$ at $b_{\max}$. On the other hand, the values of $g_2$ and $\bar{g}_2$ represent the size of nonperturbative power corrections. Therefore, sensitivity on the $g_2$ and $\bar{g}_2$ in this formalism clearly indicates the precision of the calculated $p_T$ distributions.

The solid line in Fig. 1 is the result of the QZ parameterization with $b_{\max} = 0.5$ GeV$^{-1}$ and $g_2 = \bar{g}_2 = 0$. Unlike in the $b_*$ formalism, the solid line represents the full perturbative calculation and is independent of the nonperturbative parameters for $b < b_{\max}$. The difference between the solid line and the other curves in the small $b$ region, which can be as

large as 40%, indicates the uncertainties introduced by the $b_*$ formalism.

It is clear from the solid line in Fig. 1 that there is a saddle point in the perturbative region even for the dilepton mass as low as $M = 5$ GeV in Drell–Yan production at $\sqrt{s} = 5.5$ TeV. At that energy, $x_A, x_B \sim 0.0045$. For such small values of $x$, the PDFs have very strong scaling violation, which leads to a large parton shower. It is the large parton shower at the small $x$ that strongly suppresses the function $W(b, c/b, x_A, x_B)$ in Eq. (4) as $b$ increases. Therefore, for a $b_{\max} \sim$ (a few GeV)$^{-1}$, the predictive power of the $b$-space resummation formalism depends on the relative size of contributions from the small-$b$ ($b < b_{\max}$) and large-$b$ ($b > b_{\max}$) regions of the $b$-integration in Eq. (3). With a narrow $b$ distribution peaked within the perturbative region for the integrand, the $b$-integration in Eq. (4) is dominated by the small-$b$ region, and therefore, we expect pQCD to have good predictive power even for low-$M$ Drell–Yan production at LHC energies.

Fig. 2 presents our prediction to the fully differential cross section $d\sigma/dM^2\,dy\,dp_{\mathrm{T}}^2$ for Drell–Yan production in pp collisions at $\sqrt{s} = 5.5$ TeV. Three curves represent the different order of contributions in $\alpha_s$ to the perturbatively calculated functions $\mathcal{A}(\alpha_s)$, $\mathcal{B}(\alpha_s)$, and $\mathcal{C}(\alpha_s)$ in the resummation formalism [13].

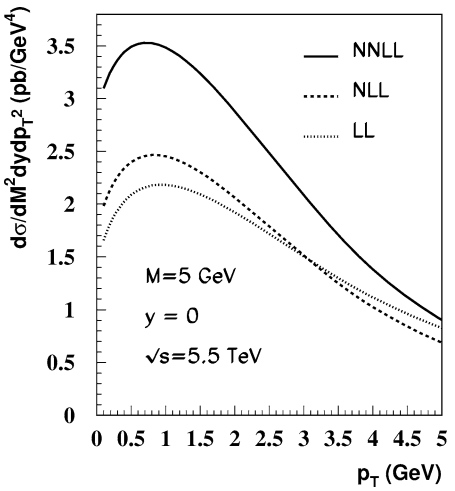


Fig. 2. Differential cross section $d\sigma/dM^2\,dy\,dp_{\mathrm{T}}^2$ for production of Drell–Yan pairs of $M = 5$ GeV in pp collisions at the LHC with $y = 0$, and $\sqrt{s} = 5.5$ TeV with the NNLL (solid), NLL (dashed), and LL (dotted) accuracy.

The solid line represents a next-to-next-to-leading-logarithmic (NNLL) accuracy corresponding to keeping the functions, $\mathcal{A}(\alpha_s)$, $\mathcal{B}(\alpha_s)$, and $\mathcal{C}(\alpha_s)$ to the order of $\alpha_s^3$, $\alpha_s^2$, and $\alpha_s^1$, respectively. The dashed line has a next-to-leading-logarithmic (NLL) accuracy with the functions, $\mathcal{A}(\alpha_s)$, $\mathcal{B}(\alpha_s)$, and $\mathcal{C}(\alpha_s)$ at the $\alpha_s^2$, $\alpha_s$, and $\alpha_s^0$, respectively, while the dotted line has the lowest leading-logarithmic (LL) accuracy with the functions, $\mathcal{A}(\alpha_s)$, $\mathcal{B}(\alpha_s)$, and $\mathcal{C}(\alpha_s)$ at the $\alpha_s$, $\alpha_s^0$, and $\alpha_s^0$, respectively. Similar to what was seen in the fixed order calculation, the resummed $p_{\mathrm{T}}$ distribution has a $K$-factor about 1.4–1.6 around the peak due to the inclusion of the coefficient $\mathcal{C}^{(1)}$.

In Eq. (10), in addition to the $g_1$ term from the leading power contribution of soft gluon showers, the $g_2$ term corresponds to the first power correction from soft gluon showers and the $\bar{g}_2$ term is from the intrinsic transverse momentum of the incident parton. The numerical values of $g_2$ and $\bar{g}_2$ have to be obtained by fitting the data. From the fitting of low energy Drell–Yan data and heavy gauge boson data at the Tevatron, we found that the intrinsic transverse momentum term dominates the power corrections and it has a weak energy dependence. For convenience, we combine the parameters of the $b^2$ term as $G_2 = g_2 \ln(M^2 b_{\max}^2/c^2) + \bar{g}_2$. For $M = 5$ GeV and $y = 0$, we use $G_2 \sim 0.25$ in the discussion here [3]. To test the $G_2$ dependence of our calculation, we define

$$R_{G_2}(p_{\mathrm{T}}) \equiv \frac{d\sigma^{(G_2)}_{AB\to l\bar{l}(M)X}(p_{\mathrm{T}})}{dM^2\,dy\,dp_{\mathrm{T}}^2} \times \left[\frac{d\sigma_{AB\to l\bar{l}(M)X}(p_{\mathrm{T}})}{dM^2\,dy\,dp_{\mathrm{T}}^2}\right]^{-1}, \tag{11}$$

where the numerator represents the result with finite $G_2$, and the denominator contains no power corrections ($G_2 = 0$).

The result for $R_{G_2}$ is shown in Fig. 3. $R_{G_2}$ deviates from unity less than 1%. The dependence of our result on the nonperturbative input is indeed very weak.

Since the $G_2$ terms represent the power corrections from soft gluon showers and partons' intrinsic transverse momentum, the smallness of the deviation of $R_{G_2}$ from unity also means that leading power contributions from gluon showers dominate the dynamics of low-mass Drell–Yan production at LHC energies. Even though the power corrections will be enhanced

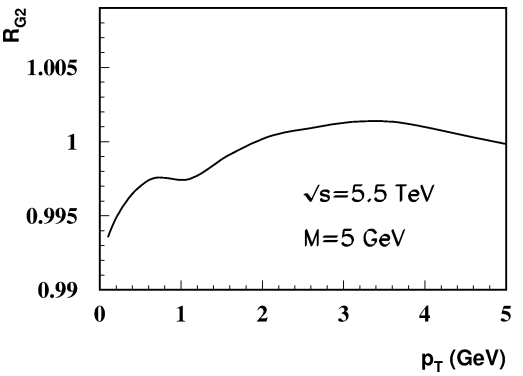


Fig. 3. The ratio $R_{G_2}$ defined in Eq. (11) with $G_2 = 0.25\ \mathrm{GeV}^2$ for the differential cross section shown in Fig. 2.

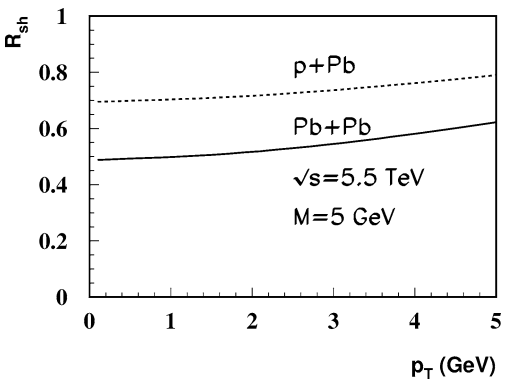


Fig. 4. $R_{\mathrm{sh}}$ as a function of $p_{\mathrm{T}}$ using EKS shadowing in Pb Pb collisions at $\sqrt{s} = 5.5$ TeV.

in nuclear collisions, we expect it to be still less than several percent [11]. The isospin effects are also small here, because $x_A$ and $x_B$ are small.

Since the leading power contributions from initial-state parton showers dominate the production dynamics, the important nuclear effect is the modification of parton distributions. Because the $x_A$ and $x_B$ are small for low-mass Drell–Yan production at LHC energies, shadowing is the only dominant nuclear effect. In order to study the shadowing effects, we define [11]

$$R_{\mathrm{sh}}(p_{\mathrm{T}}) \equiv \frac{d\sigma^{(\mathrm{sh})}_{AB\to l\bar{l}(M)X}(p_{\mathrm{T}}, Z_A/A, Z_B/B)}{dM^2\,dy\,dp_{\mathrm{T}}^2} \times \left[\frac{d\sigma_{AB\to l\bar{l}(M)X}(p_{\mathrm{T}})}{dM^2\,dy\,dp_{\mathrm{T}}^2}\right]^{-1}. \quad (12)$$

We plot in Fig. 4 the ratio $R_{\mathrm{sh}}$ as a function of $p_{\mathrm{T}}$ in p Pb and Pb Pb collisions at $\sqrt{s} = 5.5$ TeV for $M = 5$ GeV and $y = 0$. The EKS parameterizations of nuclear parton distributions [14] were used to evaluate the cross sections in Eq. (12). Fig. 4 shows that $R_{\mathrm{sh}}$ decreases about 30% from p Pb to Pb Pb collisions. It is clear that low-mass Drell–Yan production at p Pb and Pb Pb can be a good probe of nuclear shadowing.

## 4. High transverse momentum region

The gluon distribution plays a central role in calculating many important signatures at hadron colliders because of the dominance of gluon initiated subprocesses. A precise knowledge of the gluon distribution as well as its nuclear dependence is absolutely vital for understanding both hard and semihard probes at LHC energies.

It was pointed out recently that the transverse momentum distribution of massive lepton pairs produced in hadronic collisions is an advantageous source of constraints on the gluon distribution [15], free from the experimental and theoretical complications of photon isolation that beset studies of prompt photon production [16,17]. Other than the difference between a virtual and a real photon, the Drell–Yan process and prompt photon production share the same partonic subprocesses. Similar to prompt photon production, the lowest-order virtual photon "Compton" subprocess: $g + q \to \gamma^* + q$ dominates the $p_{\mathrm{T}}$ distribution when $p_{\mathrm{T}} > M/2$, and the next-to-leading order contributions preserve the fact that the $p_{\mathrm{T}}$ distributions are dominated by gluon initiated partonic subprocesses [15].

There is a phase space penalty associated with the finite mass of the virtual photon, and the Drell–Yan factor $\alpha_{\mathrm{em}}/(3\pi M^2) < 10^{-3}/M^2$ in Eq. (1) renders the production rates for massive lepton pairs small at large values of $M$ and $p_{\mathrm{T}}$. In order to enhance the Drell–Yan cross section while keeping the dominance of the gluon initiated subprocesses, it is useful to study lepton pairs with low invariant mass and relatively large transverse momentum [5]. With the large transverse momentum $p_{\mathrm{T}}$ setting the hard scale of the collision, the invariant mass of the virtual photon $M$ can be small, as long as the process can be identified exper-

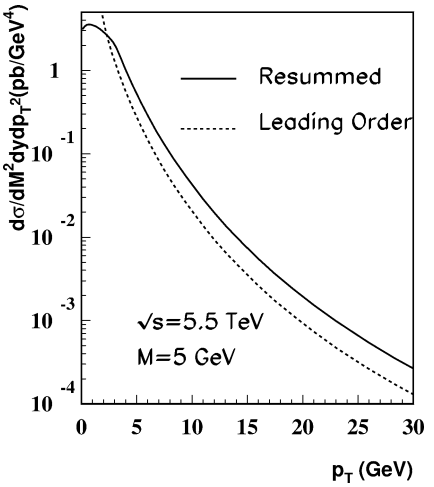


Fig. 5. Differential cross section $d\sigma/dM^2\,dy\,dp_{\mathrm{T}}^2$ for production of Drell–Yan pairs of $M = 5$ GeV in pp collisions at $\sqrt{s} = 5.5$ TeV with low and high $p_{\mathrm{T}}$ resummation (solid), in comparison to conventional lowest result (dashed).

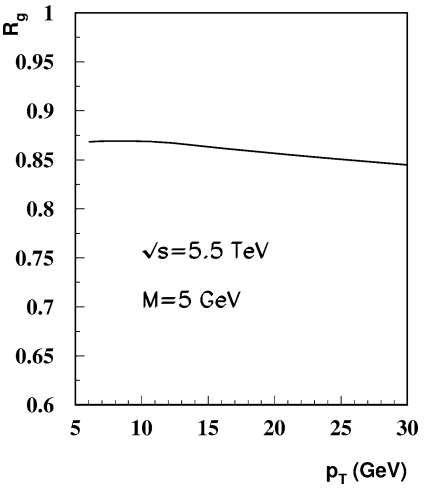


Fig. 6. Ratio of gluonic over total contributions to Drell–Yan production at the LHC, $R_g$, defined in Eq. (15) with $M = 5$ GeV at $\sqrt{s} = 5.5$ TeV.

imentally, and the numerical value $M \gg \Lambda_{\mathrm{QCD}}$. For example, the cross section for Drell–Yan production was measured by the CERN UA1 Collaboration [18] for virtual photon mass $M \in [2m_\mu, 2.5]$ GeV.

When $p_{\mathrm{T}}^2 \gg M^2$, the perturbatively calculated short-distance partonic parts, $d\hat{\sigma}_{ab\to\gamma^* X}/dp_{\mathrm{T}}^2 dy$ in Eq. (1), receive one power of the logarithm $\ln(p_{\mathrm{T}}^2/M^2)$ at every order of $\alpha_s$ beyond the leading order. At sufficiently large $p_{\mathrm{T}}$, the coefficients of the perturbative expansion in $\alpha_s$ will have large logarithmic terms, and these high order corrections may not be small. In order to derive reliable QCD predictions, resummation of the logarithmic terms $\ln^m(p_{\mathrm{T}}^2/M^2)$ must be considered. It was recently shown [5] that the large $\ln^m(p_{\mathrm{T}}^2/M^2)$ terms in low-mass Drell–Yan cross sections can be systematically resummed into a set of perturbatively calculable virtual photon fragmentation functions [19], and similar to Eq. (2), the differential cross section for low-mass Drell–Yan production at large $p_{\mathrm{T}}$ can be reorganized as

$$\frac{d\sigma_{AB\to l\bar{l}(M)X}}{dM^2\,dy\,dp_{\mathrm{T}}^2} = \frac{d\sigma^{(\mathrm{resum})}_{AB\to l\bar{l}(M)X}}{dM^2\,dy\,dp_{\mathrm{T}}^2} + \frac{d\sigma^{(\mathrm{Dir})}_{AB\to l\bar{l}(M)X}}{dM^2\,dy\,dp_{\mathrm{T}}^2}, \tag{13}$$

where $\sigma^{(\mathrm{resum})}$ includes the large logarithms and can be factorized as [5]

$$\frac{d\sigma^{(\mathrm{resum})}_{AB\to l\bar{l}(M)X}}{dM^2\,dy\,dp_{\mathrm{T}}^2} = \left(\frac{\alpha_{\mathrm{em}}}{3\pi M^2}\right)\sum_{a,b,c}\int dx_1\,\phi_{a/A}(x_1,\mu) \times \int dx_2\,\phi_{b/B}(x_2,\mu) \times \int \frac{dz}{z^2}\frac{d\hat{\sigma}_{ab\to cX}}{dp_{c\mathrm{T}}^2\,dy}(p_{c\mathrm{T}} = p_{\mathrm{T}}/z) \times D_{c\to\gamma^* X}\big(z,\mu_{\mathrm{F}}^2;M^2\big), \tag{14}$$

with the factorization scale $\mu$ and fragmentation scale $\mu_{\mathrm{F}}$, and the virtual photon fragmentation functions $D_{c\to\gamma^*}(z,\mu_{\mathrm{F}}^2;Q^2)$. The $\sigma^{(\mathrm{Dir})}$ term plays the same role as $\sigma^{(\mathrm{Y})}$ term in Eq. (2), and it dominates the cross section when $p_{\mathrm{T}} \to M$.

Fig. 5 presents the fully resummed transverse momentum spectra of low-mass Drell–Yan production in pp collisions with $M = 5$ GeV at $y = 0$ and $\sqrt{s} =$ 5.5 TeV (solid). For comparison, we also plotted the leading order spectra calculated in conventional fixed order pQCD. The fully resummed distribution is larger in the large $p_{\mathrm{T}}$ region and smoothly convergent as $p_{\mathrm{T}} \to 0$. In addition, as discussed in Ref. [5], the resummed differential cross section is much less sensitive to the changes of renormalization, factorization, and fragmentation scales, and should be more reliable than the fixed order calculations.

To demonstrate the relative size of gluon initiated contributions, we define the ratio

$$R_g = \frac{d\sigma_{AB\to\gamma^*(M)X}(\text{gluon-initiated})}{dp_{\mathrm{T}}^2\,dy} \times \left[\frac{d\sigma_{AB\to\gamma^*(M)X}}{dp_{\mathrm{T}}^2\,dy}\right]^{-1}. \quad (15)$$

The numerator includes the contributions from all partonic subprocesses with at least one initial-state gluon, and the denominator includes all subprocesses.

In Fig. 6, we show $R_g$ as a function of $p_{\mathrm{T}}$ in pp collisions at $y = 0$ and $\sqrt{s} = 5.5$ TeV with $M = 5$ GeV. It is clear from Fig. 6 that gluon initiated subprocesses dominate the low-mass Drell–Yan cross section and that low-mass Drell–Yan lepton-pair production at large transverse momentum is an excellent source of information on the gluon distribution [5]. The slow falloff of $R_g$ at large $p_{\mathrm{T}}$ is related to the reduction of phase space and the fact that cross sections are evaluated at larger values of the partons' momentum fractions.

## 5. Conclusions

In summary, we present the fully differential cross section of low-mass Drell–Yan production calculated in QCD perturbation theory with all-order resummation. For $p_{\mathrm{T}} \ll M$, we use CSS $b$-space resummation formalism to resum the large logarithmic contributions as singular as $\ln^m(M^2/p_{\mathrm{T}}^2)/p_{\mathrm{T}}^2$ to all orders in $\alpha_s$. We show that the resummed $p_{\mathrm{T}}$ distribution of low-mass Drell–Yan pairs at LHC energies is dominated by the perturbatively calculable small $b$-region and thus reliable for $p_{\mathrm{T}}$ as small as $\Lambda_{\mathrm{QCD}}$. Because of the dominance of small $x$ PDFs, the low-mass Drell–Yan cross section is a good probe of the nuclear dependence of parton distributions. For $p_{\mathrm{T}} \gg M$, we use a newly derived QCD factorization formalism [5] to resum all orders of $\ln^m(p_{\mathrm{T}}^2/M^2)$ type logarithms. We show that almost 90% of the low-mass Drell–Yan cross sections at LHC energies is from gluon initiated partonic subprocesses. Therefore, the low-mass Drell–Yan cross section at $p_{\mathrm{T}} > M$ is an advantageous source of information on the gluon distribution and its nuclear dependence—shadowing. Unlike other probes of gluon distributions, low-mass Drell–Yan does not have the problem of isolation cuts associated with direct photon production at collider energies, and does not have the hadronization uncertainties of $J/\psi$ and charm production. Moreover, the precise information on dilepton production from the Drell–Yan channel is critical for studying charm production at LHC energies.

## Acknowledgements

This work was supported in part by the US Department of Energy under Grant Nos. DE-FG02-86ER-40251 and DE-FG02-87ER-40371.

## References

[1] X.F. Zhang, G. Fai, Phys. Lett. B 545 (2002) 91.
[2] J.C. Collins, D.E. Soper, G. Sterman, Adv. Ser. High Energy Phys. 5 (1988) 1.
[3] J.W. Qiu, X.F. Zhang, Phys. Rev. Lett. 86 (2001) 2724.
[4] F. Landry, R. Brock, G. Ladinsky, C.P. Yuan, Phys. Rev. D 63 (2001) 013004, and references therein.
[5] E.L. Berger, J.W. Qiu, X.F. Zhang, Phys. Rev. D 65 (2002) 034006.
[6] J.C. Collins, D.E. Soper, G. Sterman, Nucl. Phys. B 250 (1985) 199.
[7] E.L. Berger, J.W. Qiu, Phys. Rev. D (in press), hep-ph/0210135.
[8] C.T. Davies, B.R. Webber, W.J. Stirling, Nucl. Phys. B 256 (1985) 413.
[9] G.A. Ladinsky, C.P. Yuan, Phys. Rev. D 50 (1994) 4239.
[10] F. Landry, R. Brock, P.M. Nadolsky, C.P. Yuan, hep-ph/0212159.
[11] X. Zhang, G. Fai, Phys. Rev. C 65 (2002) 064901.
[12] H.L. Lai, et al., Eur. Phys. J. C 12 (2000) 375.
[13] W. Giele, et al., hep-ph/0204316.
[14] K.J. Eskola, V.J. Kolhinen, C.A. Salgado, Eur. Phys. J. C 9 (1999) 61.
[15] E.L. Berger, L.E. Gordon, M. Klasen, Phys. Rev. D 58 (1998) 074012.
[16] E.L. Berger, J.W. Qiu, Phys. Rev. D 44 (1991) 2002.
[17] E.L. Berger, X.F. Guo, J.W. Qiu, Phys. Rev. D 54 (1996) 5470.
[18] C. Albajar, et al., UA1 Collaboration, Phys. Lett. B 209 (1988) 397.
[19] J.W. Qiu, X.F. Zhang, Phys. Rev. D 64 (2001) 074007.